Rare Metal Materials and Engineering
Volume 46, Issue 12, December 2017
Online English edition of the Chinese language journal

Cite this article as: Rare Metal Materials and Engineering, 2017, 46(12): 3601-3605.

ARTICLE

Hydrothermal Synthesis and Phase Transition Properties of Uniform Free-standing Vanadium Dioxide Nanowires

Ji Haining, Liu Dongqing, Cheng Haifeng, Zhang Chaoyang, Yang Lixiang, Zheng Wenwei

Science and Technology on Advanced Ceramic Fibers and Composites Laboratory, National University of Defense Technology, Changsha 410073, China

Abstract: Vanadium dioxide (VO_2) undergoes a Mott metal-insulator transition (MIT) close to room temperature, and has been suggested as a candidate for use in smart window and adaptive infrared camouflage. Here we report the synthesis of uniform free-standing VO_2 nanowires using a novel hydrothermal method. The synthetic nanowires have typical diameters of 150±30 nm and lengths of tens of micrometer. These VO_2 nanowires exhibit high crystallinity and a pure monoclinic phase, which were characterized by X-ray diffraction, X-ray photoelectron spectroscopy, high resolution transmission electron microscopy and selected area electron diffraction. Moreover, reversible phase transition properties of VO_2 nanowires are monitored via differential scanning calorimetry, variable temperature X-ray diffraction and temperature-dependent Raman spectroscopy. The results show VO_2 nanowires obtained exhibit a reversible phase transition with an endothermic phase transition at 65.2 ℃ and a narrow hysteresis width of 6.5 ℃. These VO_2 nanowires should be promising materials for fundamental investigations of nanoscale metal-insulator transitions.

Key words: vanadium dioxide; nanowires; hydrothermal; phase transition

Vanadium dioxide (VO_2) is one of the most interesting materials owing to its orders-of-magnitude first-order metal-insulator transition (MIT) at a temperature slightly above room temperature (T_c=68 ℃)[1]. This fortunate circumstance has inspired considerable interest in device architectures that can take advantage of the abrupt switching of electrical and optical properties accompanying this phase transition [2]. Exploiting these switching behaviors across the MIT, a number of applications have been demonstrated or proposed in smart window[3-5], optical switches[6-8], Mott transistors[9,10], strain sensors [11-13], and adaptive thermal camouflage [14-17]. One-dimensional (1D) VO_2 nanowires have attracted a great interest as building blocks used for the fabrication of nanodevices, which triggers a wide range of subsequent research in searching for newer synthetic methods. There have been many existing preparative techniques for this material. Among them, a vapor transport and thermal evaporation are the two major vapor methods to fabricate one-dimensional VO_2 nanowires[18-23]. In addition to these techniques, it is well conceived that preparation of VO_2 nanowires via solution chemical routes provides a promising option for large-scale production of this material. Although they have long been used for VO_2 single-crystal nanowires growth[2,24-29], wet-chemical approaches still face the problems of polydispersity and complicated processes in post-synthesis heating treatment. Very recently, single crystalline VO_2(A) nanowires were synthesized by a hydrothermal method using oxalic acid as reducing agent and polyethylene glycol 6000 as surfactant[30]. Although high quality VO_2 (A) nanowires have been obtained, the reported method requires an additional surfactant as additive and cannot produce single-shaped and well-crystallized morphology. Therefore, it is still a

---

Received date: December 14, 2016
Foundation item: National Natural Science Foundation of China (51502344)

Corresponding author: Cheng Haifeng, Ph. D., Professor, Science and Technology on Advanced Ceramic Fibers and Composites Laboratory, National University of Defense Technology, Changsha 410073, P. R. China, Tel: 0086-731-84576440, E-mail: chf_cfc_nudt@163.com

meaningful challenge to develop a novel approach for producing uniform free-standing VO_2 nanowires in aqueous solution.

In the present work, we report a novel one-step hydrothermal method to synthesize uniform VO_2 nanowires with a significant advance in representing the first case for directly synthesizing VO_2 nanowires without additional surfactant as additive. Furthermore, the phase-transition properties of VO_2 nanowires were studied via variable temperature X-ray diffraction (XRD) and temperature dependent Raman spectroscopy.

1 Experiment

All reagents were purchased from Aladdin chemical reagent corporation and used without further purification. VO_2 nanowires were prepared by a novel one-step hydrothermal method using a vanadium source of V_2O_5 and a reducing agent of stearic acid without additional surfactant as additive. In a typical synthesis, 1.82 g Vanadium pentoxide (V_2O_5, analytically pure) and 8.54 g stearic acid ($C_{18}H_{36}O_2$, analytically pure) were dispersed in 60 mL deionized water. The mixture was stirred for 30 min and then transferred to a 100 mL Teflon-lined stainless-steel autoclave. The hydrothermal reaction was carried out at 260 ℃ for 24 h and then air-cooled to room temperature. The final products were collected via centrifugation, washed with acetone and ethanol three times and dried in a vacuum drying oven at 80 ℃ for 10 h.

Powder XRD characterization of the prepared materials was performed using monochromatic Cu Kα radiation with a D8ADVANCE diffractometer (Bruker, Germany). Infrared absorption spectra were recorded with a Bruker Vertex 70 FTIR instrument using KBr pellet method. The morphology was obtained using a field-emission scanning electron microscope (FESEM, NOVA NanoSEM 230). The microstructure of the samples was further analyzed using a transmission electron microscopy (TEM, JEOL2010) with a LaB6 source operating at an acceleration voltage of 200 kV. Selected area electron diffraction experiments were carried out in vacuum in a JEOL 2100 transmission electron microscope working at 200 kV. X-ray photoelectron spectroscopy (XPS) data were obtained with an ESCALab220i-XL electron spectrometer from VG Scientific using 300 W Al Kα radiation. The phase transition behaviors of the resulting products were measured by differential scanning calorimetry (DSC1, METTLER TOLEDO) over the temperature range from 0 to 100 ℃ using a liquid nitrogen cooling unit. The heating and cooling rates were set at 10 ℃/min.

Variable temperature XRD data were obtained using a diffractometer (Rigaku TTR-III) equipped with a with a Cu Kα radiation (λ=0.15418 nm). Under steady N_2 flow, the sample was heated (from 30 ℃ to 70 ℃) and cooled (from 70 ℃ to 30 ℃) inside a Rigaku Reactor-X chamber fitted with a Beryllium window. Temperature dependent Raman spectroscopy was recorded using a Horiba JY HR Evolution Spectroscopy System. The excitation wavelength is 532 nm, with laser power kept at 1 mW to ensure that thermal heating due to the laser focusing does not trigger the MIT. External sample temperature was controlled via a programmable heating- cooling stage.

2 Materials and Methods

2.1 Characterization

The XRD pattern of a sample obtained at 260 ℃ for 24 h is shown in Fig.1a as a representative. All peaks can be indexed as a single monoclinic phase VO_2 (M) (JCPDS. Card. No. 43-1051). It can also be seen that all of the peaks are sharp and strong with relatively narrow peak widths, indicating the good crystallinity of VO_2 (M). The results indicate that phase-pure and well-crystallized VO_2 (M) nanowires can be synthesized by such a novel one-step hydrothermal method.

To investigate the chemical bonding between vanadium and oxygen ions and to confirm the phase purity, we performed FTIR spectrum measurement. Fig.1b shows the FTIR spectrum of VO_2 (M) sample prepared. The main vibrational bands observed from the FTIR spectrum are at 995, 735, 524, 433 cm^{-1} and can be considered as intrinsic to vanadium dioxide, which matches well with earlier reports: the initial broad vibrational band at 524 cm^{-1} and 433 cm^{-1} are assigned to the V-O-V octahedral bending modes; the band at 995 cm^{-1} and 735 cm^{-1} is attributed to the coupled vibration of V═O [31-34]. These FTIR observations confirm that the nanowires correspond to the VO_2 phase.

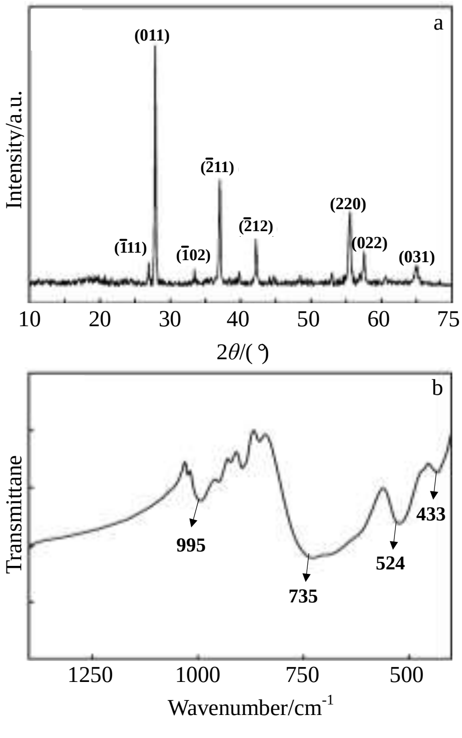

Fig.1 XRD patterns acquired for as-synthesized VO_2 nanowires (a) and FTIR spectrum of VO_2 sample prepared (b)

As shown in Fig. 2, the composition of the VO_2 sample is further characterized by XPS. A typical XPS spectrum for the VO_2 sample indicates the existence of V, O and C elements, where the carbon is attributed to surface contamination (Fig. 2a). From Fig. 2b, it could be found that the V $2p_{3/2}$ peak of the nanowires is centered at 515.9 eV in good agreement with 516.0 eV of pure VO_2[35]. The difference in the binding energy between O 1s and V $2p_{3/2}$ was 14.1 eV, corresponding to that value of literature[36, 37] (14.0~14.2 eV). Fig.2c shows the Al Kα valence band photoemission spectra for VO_2 sample. The spectrum of VO_2 has been shifted in energy to place the Fermi level at the top of the known small energy gap, since the VO_2 sample shows strong charging effects during the measurements at room temperature [38, 39]. Combined with XRD, the data of XPS provides an effective evidence of no other vanadium valences in VO_2 (M).

The SEM images of the sample in Fig.3a and 3b reveal strikingly unique wire morphology with typical diameters of 150±30 nm and lengths of tens of micrometer. Lattice resolved HRTEM images (Fig.3c) and the selected area electron diffraction (SAED) patterns (Fig. 3d) of an individual nanowire corroborate the phase assignment to the monoclinic phase of VO_2. The interplanar spacing is calculated to be around 0.332 and 0.484 nm, which is indexed to the (-111) and (100) facets of VO_2 (M). SAED patterns in Fig.3d reveal that the VO_2 nanowires could be indexed to VO_2 (M), which is consistent with XRD patterns.

2.2 Phase transition

The fully reversible phase transition of the as-synthesized VO_2 (M) nanowires are clearly revealed by DSC curves, variable temperature XRD and temperature-dependent Raman spectroscopy. Fig.4a illustrates that the VO_2 (M) nanowires display a thermal hysteresis phenomenon with a width of 6.5 ℃, which is narrower than the results reported in the literature[40,41]. This may be caused by the interface effects[42]. The heating of the VO_2 (M) nanowires is accompanied by endothermal effects at 65.2 ℃ in the DSC curves, corresponding to the transition temperature of VO_2 from the monoclinic phase VO_2 (M) to the tetragonal phase VO_2 (R) (see schematic in Fig.4b). Accordingly, the thermal analysis results provide the direct evidence for the occurrence of temperature driven first-order phase transition in VO_2 (M) nanowires. Furthermore, the structural phase transition is directly detected using the variable temperature XRD patterns in Fig.5a and 5b. For example, the diffraction peak clearly changes on going from the low-temperature VO_2 (M) phase $(011)_m$ peak to the high-temperature VO_2 (R) phase $(110)_r$ peak and then to the low-temperature VO_2 (M) phase $(011)_m$ peak. Obviously, VO_2 (M) can transform to VO_2 (R) at 70 ℃. This result is nearly consistent with our DSC findings. The metal-insulator transition of VO_2 is also verified by the corresponding temperature-dependent Raman spectroscopy in Fig.5c. The low-temperature (30 ℃) Raman spectra with

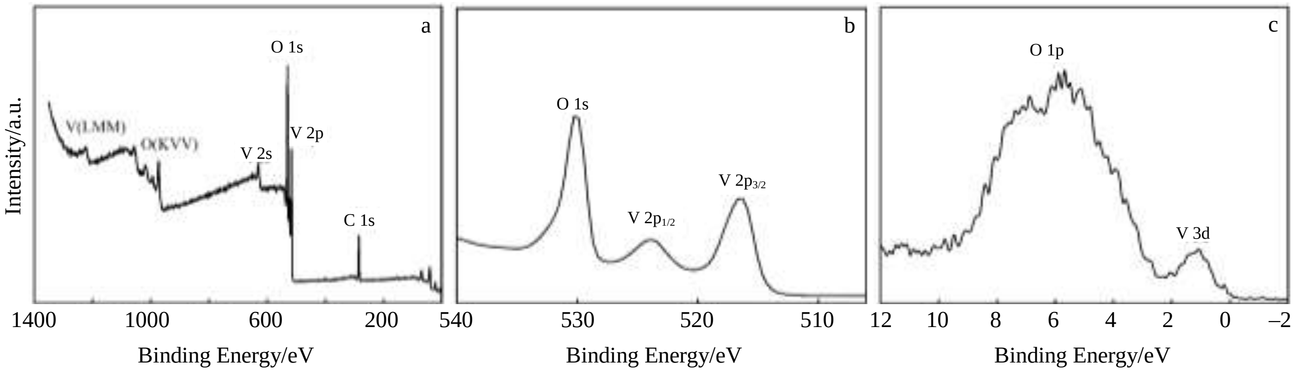

Fig. 2 XPS survey spectra of VO_2 sample (a), core-level spectrum of VO_2 sample containing V 2p and O 1s (b), valence band XPS spectra of VO_2 sample (c) taken at room temperature

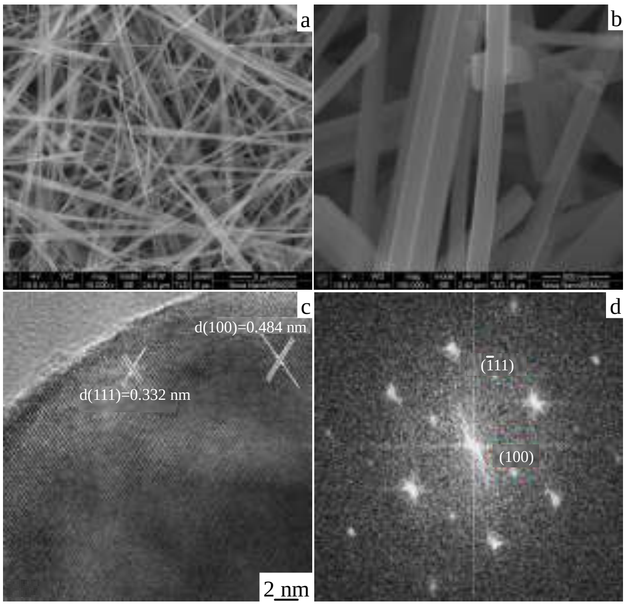

Fig. 3 SEM images (a, b), HRTEM image (c), and SAED patterns (d) of monoclinic VO_2 nanowires

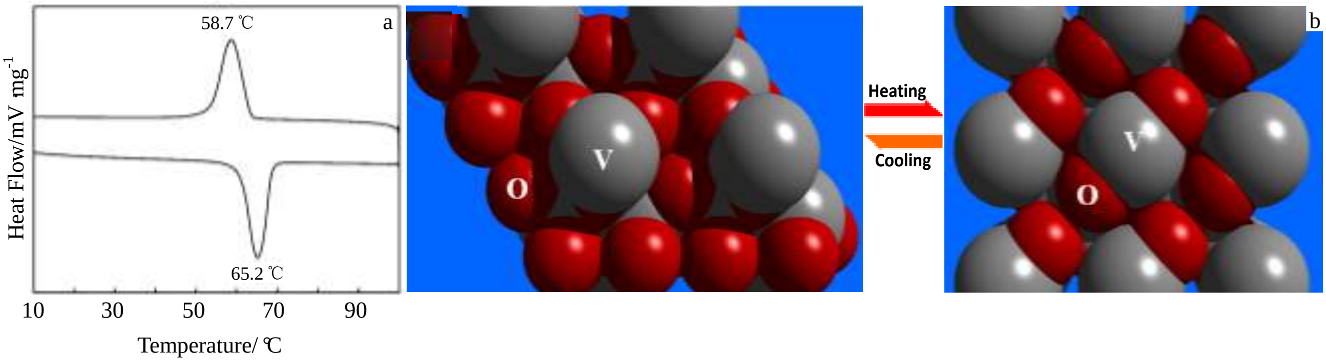

Fig.4 DSC curves of VO_2 (M) nanowires (a) and schematic of phase evolution between monoclinic VO_2 (M) and tetragonal rutile VO_2 (R) (b)

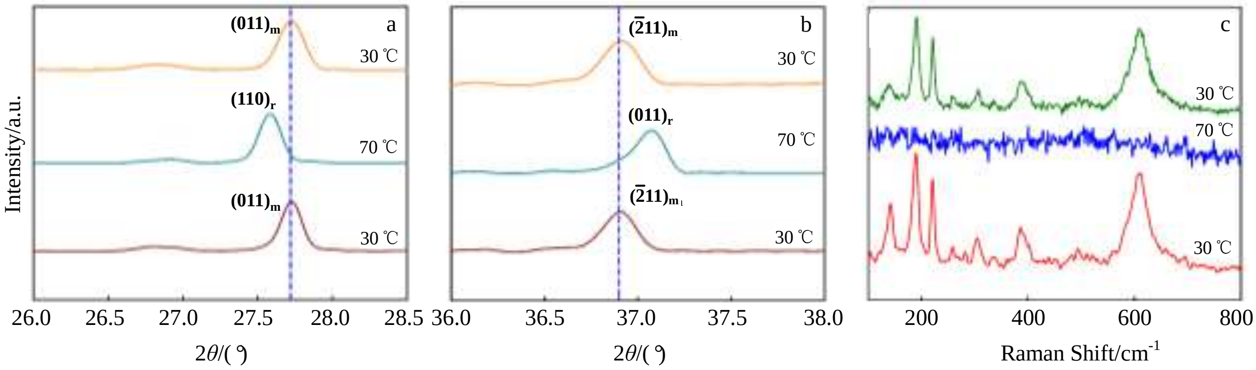

Fig.5 Variable temperature XRD patterns in diffraction angle of 26.0~28.5 °(a), variable temperature XRD patterns in diffraction angle of 36.0~38.0 °(b), and temperature-dependent Raman spectroscopy (c)

peaks at 142, 190, 222, 259, 306, 339, 388, 440, 497, and 613 cm^{-1} could be assigned to the as-obtained VO_2(M) nanowires[20, 43-44]. When the temperature rises to 70 ℃, these Raman peaks vanish due to the transformation into VO_2 (R). However, when the temperature is reduced to 30 ℃, Raman peaks appears again. Therefore, the evolution of Raman spectra as a function of temperature further evidences the reversible phase transition between VO_2 (M) and VO_2 (R) nanowires.

3 Conclusions

1) Uniform free-standing VO_2 nanowires can be synthesized via a novel hydrothermal process using a vanadium source of V_2O_5 and a reducing agent of stearic acid without additional surfactant as additive.

2) The synthetic VO_2 nanowires exhibit high crystallinity and feature a pure monoclinic phase and composition.

3) VO_2 nanowires obtained exhibit a reversible monoclinic to tetragonal structural transition with a metal-insulator transition at 65.2 ℃ and a narrow hysteresis width of 6.5 ℃.

4) The distinct structural transition between VO_2 (M) and VO_2 (R) nanowires is further verified by the corresponding variable temperature XRD and temperature-dependent Raman spectroscopy, which would help us understand the mechanism on phase transition for the advanced applications of VO_2-based nanodevices.

References

1 Eyert V. *Annalen Der Physik*[J], 2002, 11: 650

2 Horrocks G A, Singh S, Likely M F *et al. ACS Applied Materials & Interfaces*[J], 2014, 6: 15 726

3 Zhou J D, Gao Y F, Zhang Z T *et al. Scientific Reports*[J], 2013(3): 3029

4 Gao Y F, Luo H J, Zhang Z T *et al. Nano Energy*[J], 2012(1): 221

5 Warwick M E A, Binions R. *Journal of Materials Chemistry A*[J], 2014(2): 3275

6 Makarevich A M, Sadykov I I, Sharovarov D I *et al. Journal of Materials Chemistry C*[J], 2015(3): 9197

7 Zhang Y F, Zhang J C, Zhang X Z *et al. Materials Letters*[J], 2013, 92: 61

8 Zhang Y B, Huang W X, Song L W *et al. Journal of Inorganic Materials*[J], 2013, 28: 229

9 Ji H, Wei J, Natelson D. *Nano Letters*[J], 2012, 12: 2988

10 Hormoz S, Ramanathan S. *Solid-State Electronics*[J], 2010, 54: 654

11 Wu C Z, Feng F, Xie Y. *Chemical Society Reviews*[J], 2013, 42: 5157

12 Li S T, Li Y M, Jiang M *et al. ACS Applied Materials & Interfaces*[J], 2013(5): 6453
13 Cao J, Ertekin E, Srinivasan V *et al. Nature Nanotechnology*[J], 2009(4): 732
14 Xiao L, Ma H, Liu J *et al. Nano Letters*[J], 2015, 15: 8365
15 Mao Z P, Wang W, Liu Y *et al. Thin Solid Films*[J], 2014, 558: 208
16 Kats M A, Blanchard R, Zhang S Y *et al. Physical Review X*[J], 2013(3): 041 004
17 Ji H N, Liu D Q, Cheng H F *et al. RSC Advances*[J], 2017(7): 5189
18 Guiton B S, Gu Q, Prieto A L *et al. Journal of the American Chemical Society*[J], 2005, 127: 498
19 Cheng C, Liu K, Xiang B *et al. Applied Physics Letters*[J], 2012, 100: 103 111
20 Cheng C, Guo H, Amini A *et al. Scientific Reports*[J], 2014(4): 5456
21 Strelcov E, Lilach Y, Kolmakov A. *Nano Letters*[J], 2009(9): 2322
22 Sohn J I, Joo H J, Porter A E *et al. Nano Letters*[J], 2007(7): 1570
23 Kim I S, Lauhon L J. *Crystal Growth & Design*[J], 2012, 12: 1383
24 Gui Z, Fan R, Mo W *et al. Chemistry of Materials*[J], 2002, 14: 5053
25 Yin H, Luo M, Yu K *et al. ACS Applied Materials & Interfaces*[J], 2011(3): 2057
26 Liu J F, Li Q H, Wang T H *et al. Angewandte Chemie International Edition*[J], 2004, 43: 5048
27 Sung-Hwan B, Sangmin L, Hyun K *et al. Advanced Materials*[J], 2013, 25: 5098
28 Mai L Q, Hu B, Hu T *et al. Journal of Physical Chemistry B*[J], 2006, 110: 19 083
29 Pan M, Zhong H, Wang S *et al. Journal of Crystal Growth*[J], 2004, 265: 121
30 Liu X, Xiong W, Zheng Y. *International Conference on Mechanics, Materials and Structural Engineering*[C]. Jaeju-Do, South Korea: ICMMSE, 2016: 1
31 Popuri S R, Miclau M, Artemenko A *et al. Inorganic Chemistry* [J], 2013, 52: 4780
32 Sediri F, Gharbi N. *Materials Science and Engineering B-Solid State Materials for Advanced Technology*[J], 2007, 139: 114
33 Sediri F, Gharbi N, *Materials Science & Engineering B*[J], 2007, 139: 114
34 Botto I L, Vassallo M B, Baran E J *et al. Materials Chemistry & Physics*[J], 1997, 50: 267
35 Ji H N, Liu D Q, Zhang C Y *et al. Science of Advanced Materials*[J], 2017(9): 861
36 Kang L T, Gao Y F, Luo H J. *ACS Applied Materials & Interfaces*[J], 2009(1): 2211
37 Shen N, Dong B, Cao C *et al. RSC Advances*[J], 2015, 5: 108 015
38 Surnev S, Ramsey M G, Netzer F P. *Progress in Surface Science*[J], 2003, 73: 117
39 Zimmermann R, Claessen R, Reinert F *et al. Journal of Physics Condensed Matter*[J], 1998(10): 5697
40 Whittaker L, Jaye C, Fu Z G *et al. Journal of the American Chemical Society*[J], 2009, 131: 8884
41 Song Z, Zhang L, Xia F *et al. Inorganic Chemistry Frontiers*[J], 2016(3): 1035
42 Zhong L, Li M, Wang H *et al. Cryst Eng Comm*[J], 2015, 17: 5614
43 Hu B, Ding Y, Chen W *et al. Advanced Materials*[J], 2010, 22: 5134
44 Chen R, Miao L, Liu C *et al. Scientific Reports*[J], 2015(5): 14087

均匀自支撑的二氧化钒纳米线的水热合成及相变特性研究

嵇海宁，刘东青，程海峰，张朝阳，杨力祥，郑文伟
(国防科技大学 新型陶瓷纤维及其复合材料重点实验室，湖南 长沙 410073)

摘 要：二氧化钒（VO_2）在接近室温时发生由半导体态向金属态的 Mott 相变，在智能窗和红外自适应伪装技术领域具有一定的应用前景。采用一种新颖的水热法制备了均匀自支撑的 VO_2 纳米线。合成的纳米线的直径为 150±30 nm，长度达到几十微米。通过 X 射线衍射、X 射线光电子能谱、高分辨透射电镜和选取电子衍射等手段验证了高纯单斜相 VO_2 纳米线的成功制备。而且，VO_2 纳米线的可逆相变性能采用差示量热扫描、变温 XRD 和变温 Raman 光谱进行了探究。结果表明：VO_2 纳米线升温相变点为 65.2 ℃，磁滞回线宽度窄至 6.5 ℃，具有良好的可逆相变性。这些为 VO_2 纳米线的金属-半导体相变研究提供基础。

关键词：二氧化钒；纳米线；水热法；相变

作者简介：嵇海宁，男，1984 年生，博士生，国防科技大学新型陶瓷纤维及其复合材料重点实验室，湖南 长沙 410073，电话：0731-84576440，E-mail: sdytjhn@126.com